Science of the Total Environment 966 (2025) 178543

Contents lists available at ScienceDirect

Science of the Total Environment

journal homepage: www.elsevier.com/locate/scitotenv

Microplastics in Antarctica - A plastic legacy in the Antarctic snow?

Kirstie Jones-Williams [a,1], Emily Rowlands [a,*,1], Sebastian Primpke [b], Tamara Galloway [c], Matthew Cole [d], Claire Waluda [a], Clara Manno [a]

[a] British Antarctic Survey, High Cross Madingley Road, Cambridge CB3 0ET, United Kingdom of Great Britain and Northern Ireland
[b] The Alfred Wegener Institute (AWI) Alfred Wegener Institute, Kurpromenade 27498, Helgoland, Germany
[c] University of Exeter, Stocker Rd, Exeter EX4 4PY, United Kingdom of Great Britain and Northern Ireland
[d] Plymouth Marine Laboratory, Prospect Pl, Plymouth PL1 3DH, United Kingdom of Great Britain and Northern Ireland

HIGHLIGHTS

- Small MPs >11 μm were explored in Antarctic snow for the first time.
- 95 % of MPs were <50 μm, Antarctic MP may be a greater concern than previously thought.
- Polyamide dominated across sites, making up 78 % of the sample at Schanz Glacier.
- Anthropogenic activities are leaving an MP legacy in Antarctic snow.
- Results show global plastic pollution mitigation strategies are essential.

GRAPHICAL ABSTRACT

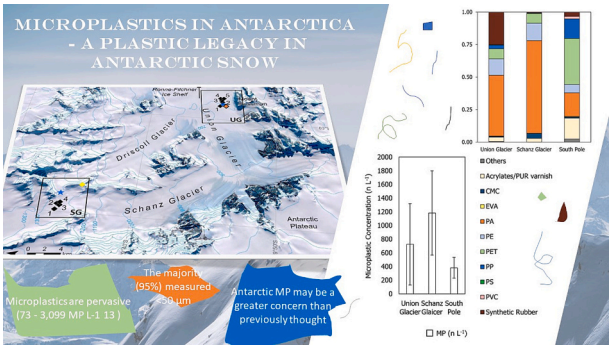

ARTICLE INFO

Editor: Frederic Coulon

Keywords:
Microplastic
Pollution
Antarctica
FTIR
Atmospheric Plastic
Snow

ABSTRACT

Microplastic pollution in remote inland Antarctica is largely unknown. This study explored the plastic footprint of snow from remote Antarctic camps: Union Glacier, Schanz Glacier and the South Pole. Refined automated FTIR techniques enabled interrogation of microplastics (including fibres) to a lower detection limit of 11 μm in Antarctic snow for the first time. Microplastics were pervasive (73–3099 MP L^{-1}). The majority (95 %) measured <50 μm, indicating that previous microplastic reports in Antarctica may be underestimated, due to analytical restrictions. Plastic polymer composition and concentration did not vary significantly between sites, with dominant polymers being polyamide (PA), polyethylene terephthalate (PET), polyethylene (PE) and synthetic rubber. Results indicate that even in the earth's most remote regions, humans are leaving a plastic legacy in the snow, illustrating the importance of remote, cryospheric regions as critical study sites for determining temporal fluxes in microplastic pollution.

* Corresponding author.
E-mail addresses: emirow@bas.ac.uk (E. Rowlands), clanno@bas.ac.uk (C. Manno).
[1] Kirstie Jones-Willaims and Emily Rowlands share joint first authorship.

https://doi.org/10.1016/j.scitotenv.2025.178543
Received 25 June 2024; Received in revised form 13 January 2025; Accepted 14 January 2025
Available online 6 February 2025
0048-9697/© 2025 The Authors. Published by Elsevier B.V. This is an open access article under the CC BY license (http://creativecommons.org/licenses/by/4.0/).

1. Introduction

Antarctica is regarded as the world's last great wilderness. Isolated by the Antarctic Circumpolar Current (ACC), it is the coldest, driest, highest, and most remote continent (Barker et al., 2007). The frozen continent has unique protection under the Antarctic Treaty System (ATS), effective since 1961 (The Antarctic Treaty | Antarctic Treaty, 2023). Human presence in Antarctica is limited to scientific research, fishing, tourism, and support for logistics with any proposed activity undergoing an environmental impact assessment (Grant et al., 2021). Despite environmental provisions, Antarctica is not immune to anthropogenic pressures. The ACC, once considered a physical barrier for pollution and invasive species, can be breached, bringing pollution to Antarctica via ocean currents (Sul et al., 2011; Fraser et al., 2016). Long-range atmospheric transport can potentially be a key mechanism for microplastic transport from populated to remote regions (Allen et al., 2020, 2022; Bergmann et al., 2019) or from the ocean (Allen et al., 2019) to remote regions including Antarctica (Aves et al., 2022). The polar regions are often considered a sink for pollutants (van Sebille et al., 2020) via atmospheric and ocean currents, however, global warming threatens the re-emergence of these contaminants from permafrost (Potapowicz et al., 2018) and sea-ice melt (Obbard et al., 2014). The presence of humans as carriers of local pollution in Antarctica potentially puts this region at even greater risk (Cai et al., 2012; Reed et al., 2018; Tejedo et al., 2022). With most permanent research stations and tourist landings occurring on the coast (COMNAP, 2022; IAATO, 2021), local point sources of pollution are understudied in the remote inland regions of Antarctica (Aves et al., 2022). However plastic pollution, which is intertwined with the Antarctic food web, can have a wide range of ecological consequences from small nanoplastics hindering the development of Antarctic krill (Rowlands et al., 2021) to microplastic debris being found in the digestive tract of a range of Antarctic seabirds which may cause gastrointestinal tract blockages, toxicity and oxidative stress (Taurozzi and Scalici, 2024).

Plastics are a diverse group of polymer-based materials, which can be physically altered in the manufacturing process (melting, extrusion, palletisation) and by incorporation of other chemicals (e.g. flame retardants, colorants, plasticisers). Once released into the environment, weathering processes such as photooxidation by ultraviolet (UV) will further alter the chemical and mechanical properties of the plastic (Galloway et al., 2017) and once below 5 mm in size, these so-called microplastics constitute a vast and diverse range of pollutants (Thompson, 2015). Whilst the Madrid Protocol determines that all plastics must be removed from Antarctica after use, or in the case of low-density polyethylene bags, incinerated (Annex III, Madrid Protocol), there currently lacks any mention of microplastics in this environmental framework. Few studies have this far been conducted on Antarctic snow. One study from Ross Island, East Antarctica used visual identification, followed by micro-Fourier transform Infrared spectroscopy (μFTIR) to identify an average of 29 particles L^{-1} in snow (Aves et al., 2022). Methods used were limited for microplastic detection to sizes >50 μm. More recently, using Raman spectroscopy polyethylene and poly (ethylene-*co*-viny-acetate) microplastics <20 μm were detected for the first time in Antarctic snow from different areas of Terra Nova Bay though concentrations were not reported (Riboni et al., 2024). Microplastics <50 μm more widely have been identified as a major component of plastic pollution in other remote regions in the Arctic (Peeken et al., 2018; Bergmann et al., 2019) as well as in urban areas (Fan et al., 2022). The footprint of humans in Antarctica may therefore be much greater than current estimates.

From its first introduction in the 1950s, there is now enough plastic pollution to form a permanent and distinct layer in the earth's fossil record (Zalasiewicz et al., 2021). However, with comparably low visible plastic pollution in Antarctica, little is known about this plastic legacy on the frozen continent. This study provides new insights into the presence of plastic pollution in the most remote, inland section of continental Antarctica with field camps, by measuring microplastics down to 11 μm in size, to test the hypothesis that microplastic reports from earlier studies in Antarctica are underestimated due to analytical restrictions.

2. Methods

2.1. Field collections

Snow samples were taken in December 2019 from three locations in Antarctica (Union Glacier, Schanz Glacier, and the South Pole) (Fig. 1). Union Glacier (79°460 S, 83°240 W) is situated at the northern edge of the Western Antarctic Ice sheet, the glacier extends 86 km up to the grounding line of the Ronne-Filchner Ice Shelf. Sitting approximately 550 m above and draining into Union Glacier 30 km away is the similarly u-shaped Schanz Glacier. The Amundsen-Scott South Pole Base and field camp is 1140 km away from Union Glacier (Fig. 1). These three sites represent different remote camps, varying in size and accessibility. Twelve sites were selected for analysis: five at Union Glacier (UG1-UG5, close to the downwind of the camp), four at Schanz Glacier (SG1-SG4, 2 km area between the tracks and the retreat), and three at the South Pole (SP1-SP3), including one at the runway (SP3) and two at 250 m intervals further from the Amundsen-Scott South Pole Base. A sample was taken at the control site chosen based on logistics as the most remote location accessible (Fig. 1), atop an exposed ridge between the Schanz and Driscoll Glacier >100 m above Schanz Glacier and unlikely to be impacted by the local camp.

The camp at Union Glacier is seasonal and is operational during the summer period between October/November and February, hosting approximately 420 people annually, housing up to a maximum of 140 people at any given time IAATO (2021). At Schanz Glacier there is a small touristic “retreat” camp which houses a maximum of 16 people. In contrast, at the South Pole, the National Science Foundation (NSF) centre, houses a maximum of 100 people in the summer with approximately 50 people overwintering, with approximately 250 people visiting the centre each year. All three sites share similar snow accumulation and annual precipitation (Hoffmann et al., 2020a, 2020b; Lazzara et al., 2012). Snow accumulation within the main Union Glacier valley (700 m above sea level) has been estimated at 0.180 (0.11–0.364) m w.e.a^{-1} (wet equivalent annually) over 30 years between 1989 and 2014 whilst snow accumulation within Schanz Glacier has been measured with an average of 0.247 (0.142–0.390) m w.e.a^{-1} (Hoffmann et al., 2020a, 2020b). Despite sitting at an altitude of 2700 m, the snow accumulation rate at the South Pole is comparable to that observed at Union and Schanz Glacier at approximately 0.274 m w.e.a^{-1} (Lazzara et al., 2012). Additional environmental parameters and the proximity of each individual sample to the nearest camp were recorded to determine whether these variables had any statistical influence on the composition and concentration of microplastics (table S1). Temperature, wind speed and wind direction were recorded using a Kestrel 5000 Environmental meter whilst precipitation conditions were described in observer notes and elevation recorded from the GPS and corroborated with topographical map data (SCAR Antarctic Digital Database). Approximate distances of proximity were measured using GIS (Fig. 1).

A shallow pit was dug using a shovel to 20–40 cm depth, and the person collecting the sample was positioned downwind of the pit (Fig. 2). Sampling was downwind of remote camps in an attempt to quantify their contribution to the microplastic footprint in the snow. The farthest wall of each pit was then “cleaned” of any potential contamination from the shovel by scraping approximately 5-10 cm of snow from the wall with a stainless-steel cup. The cup was acid-cleaned between each sample site. Snow samples were taken at between 20 and 40 cm depth, to include the variance of snow accumulation across all sites. Thus, this study assumes that sampling of this layer comprises the plastic legacy of the previous 1–2 years (Hoffmann et al., 2020a, 2020b; Lazzara et al., 2012).

A sample was taken by burrowing laterally into the side of the wall

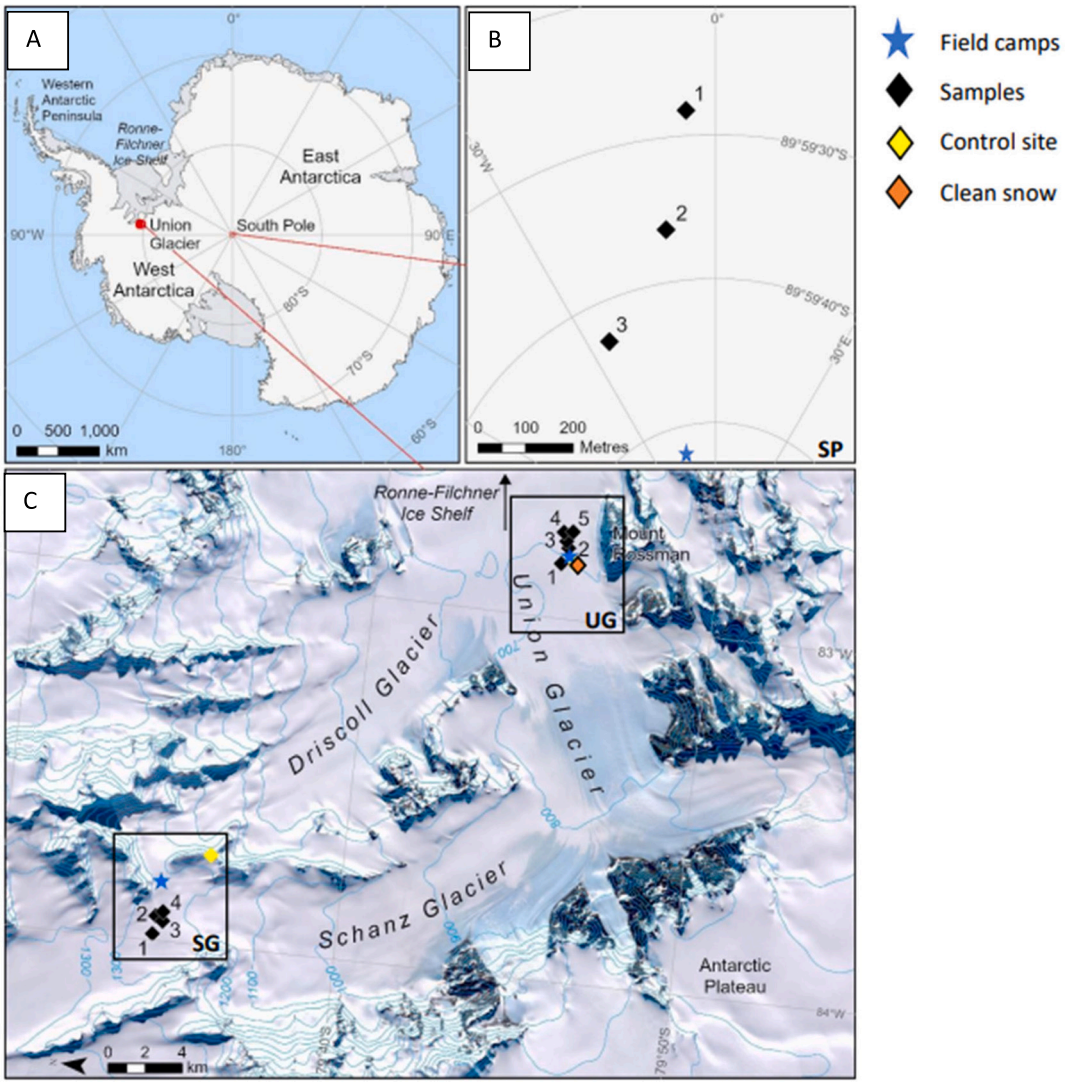

Fig. 1. Locations of the study regions relative to one another in continental Antarctica (A), and the individual sample locations at B: the South Pole (SP) and C: Union Glacier (UG) and Schanz Glacier (SG). Blue stars mark the camps. Samples are marked by black diamonds. Control sample taken near Schanz Glacier is denoted by a yellow diamond. Orange diamond to denote location of "clean snow" as referenced in field collection methods. Maps were compiled in Quantum GIS (v3.10.4). Background image (C) was extracted from the Landsat Image Mosaic of Antarctica (LIMA). Coastline and contours from the SCAR Antarctic Digital Database, accessed 2023.

using the stainless-steel cup. The first "scoop" of each tunnel was discarded, with all subsequent collections with the cup decanted into an 800 ml stainless steel tankard (ECOtanka™), which remained closed when not used and placed upwind of the sampler when being used. Each container was filled, bumping the base of the tankard to collect as much as possible, with variation in snowmelt volume recorded. Each tankard was then sealed and returned to the field laboratory for filtering.

2.2. Sample processing

In the field laboratory, samples were kept sealed and slowly melted in the tankards. Once cooled, the snowmelt was measured (Table S1) and then subsequently filtered through a 10 ml funnel onto 25 mm diameter, 5 μm pore silver filters (Sterlitech) using a glass filter system, connected to a pump via polycarbonate tube creating a vacuum. All instruments were covered with aluminium foil when not being decanted for filtration.

The funnel was flushed through with "clean water" after filtering. In place of deionised water at the camp, "Clean water" was produced using the "clean snow" supply – an area of snow sectioned off, upwind of the camp (Fig. 1), used for generating the cooking water and shower water supply at Union Glacier. This snow was collected and twice filtered through a 0.2 μm Isopore (polycarbonate) to remove any possible plastic contamination. Investigation under a stereomicroscope indicated no visible microplastic or other particulate, as expected when passing through a small pore-size filter. A sample of this "clean snow" was taken before filtering and processed as per other samples for microplastics analyses. The results of this are included in supplementary table S3.

2.3. Quality assurance

Best practice anti-contamination measures were taken in each laboratory. As the field laboratory was set up for the field campaign, it was thoroughly cleaned, and air conditioning remained off for the campaign. Footfall within the laboratory was restricted to the researcher, and cotton laboratory coats were worn. All instruments and containers were acid-washed before first use and were covered with aluminium foil during processing. At the British Antarctic Survey Laboratory - Cambridge, aluminium foil was used during filtering, and glass lids were used during the drying process. A bespoke Perspex shield was fitted

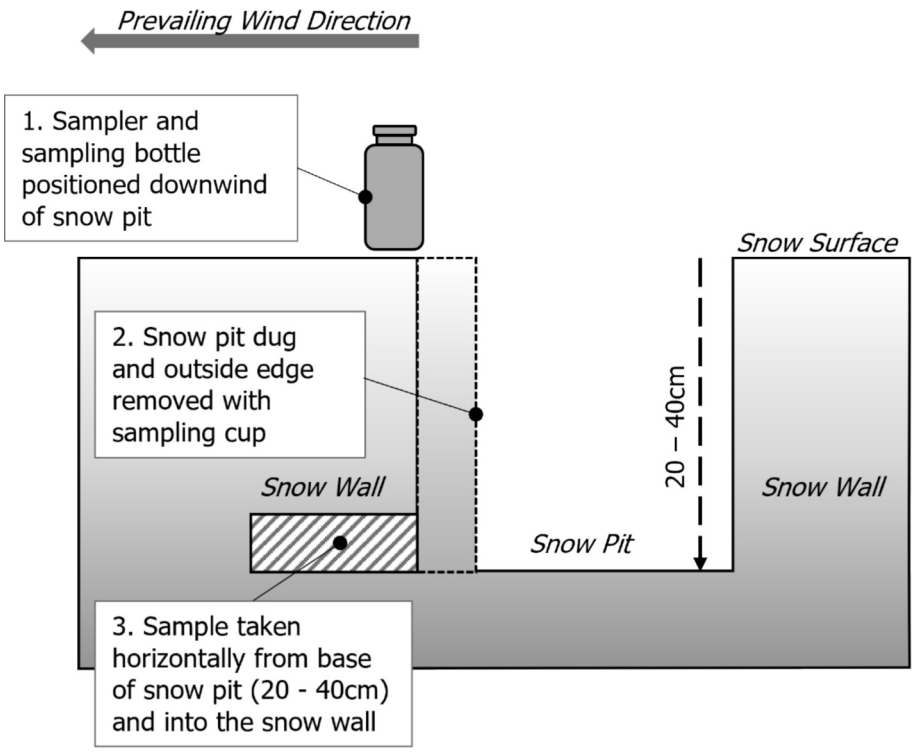

Fig. 2. Schematic illustrating the sampling protocol.

around the FTIR stage to prevent airborne contamination during infrared analysis. The laboratory was thoroughly cleaned, and surfaces were wiped down with an ethanol dilution between each sample processing and analysis. Procedural blanks were taken to measure the introduction of contamination at any of these stages and recovery tests, to measure the loss of sample during processing.

A contamination library was also built. For this, fibre samples were collected from the garments worn by each person in the field and the laboratory, with particles from additional possible sources of plastic pollution also collected from the field camp (table S5). These samples were analysed using attenuated total reflection using a mobile Agilent FTIR. Spectra were collected and measured against the existing spectral reference library using the siMPle software. Hierarchical cluster analysis was carried out according to Primpke et al. (2018) using the Hellinger Distance for the calculation of the resemblance matrix (Primer 6 and Permanova, Primer-E) was performed to identify the primary polymer composition of these samples (Table S5) by their similarity to existing database entries (Fig. S1) and inform, post-hoc, on possible sources of contamination.

Procedural blanks were run in triplicate. Two separate sets of blanks were carried out. The first type, the "Full Procedural Blank," replicated the complete procedure from collection to analysis, as per all other snow samples. A separate ECOtanka™ was used to collect 250 ml of 0.2 μm filtered "clean water" and was processed in the same manner, i.e., filtering onto a silver filter in the field laboratory and subsequently transferred onto an Anodisc® filter for FTIR analysis. Each blank was carried out on the same day the samples were processed in the field laboratory ($n = 3$). In addition, a secondary set of procedural blanks was taken to inform about contamination introduced during the transference step from silver filter to Anodisc®. These blanks, "Laboratory Blanks," replicate the procedure carried out in the Cambridge Laboratory, using 200 ml of 0.2 μm filtered Milli-Q water, filtered onto a silver filter and subsequently removed using 50 ml of Milli-Q water onto an Anodisc® and 10 ml of 30 % Ethanol to help remove any residual filtrate.

To determine the final "normalised concentration" presented in the results, the concentration of each polymer type was averaged from the three "Full Procedure" blanks and subtracted from each raw sample concentration (Fig. S1, result 1). The concentration recorded in the lab blank (Fig. S1, result 2) was used only to inform what proportion may have been introduced in the laboratory. Furthermore, the fraction likely introduced during field processing is determined by subtracting the "Lab Result" from the "Full Result" (Fig. S1, result 3).

Recovery tests were designed to determine whether there was any substantial material loss during the transference step from silver filter to Anodisc®. These recovery tests were carried out in triplicate, using Nylon fibres stained with Nile Red and had a uniform diameter of 16 μm, and cut to a length of 250 μm. A fluorescent microscope was used to count fibres once dry. Following this, the sample was enclosed in its case. It was shaken to mimic the disturbance of the sample within the case that was potentially encountered during transit. The sample was then removed, filtered onto the Anodisc® filter, and counts made again. For both counts, photographs were also taken across the entire filter to validate counts. In addition, one of the recovery tests was subsequently analysed using FTIR to compare the manual counts with those counted by the software. Average laboratory blank nylon fibres ($n = 3$) were subtracted from the final count.

2.4. Identification of microplastics using fourier transform infrared spectrometry

Detailed processing of the samples is provided (Table S2). In brief, this required samples to be removed from the silver filter and transferred onto Anodisc® filters (Whatman®) (see SI1 for full description). Three laboratory blanks were carried out to determine the possible introduction of contamination during this step and any sample loss (Fig. S1). The transfer of samples onto new filters enabled the use of the focal plane array (FPA) and full analysis of the whole filter area using Fourier Transform infrared (FTIR) in transmission mode. Initial observations using an Olympus Stereomicroscope (Fig. 3A, D) indicated that particles were either <100 μm or were MP fibres. We combined the method of Primpke et al. (2018) with technical advice provided by Agilent Technologies; and overlaid a 2 mm thick Barium Fluoride slide on top of the

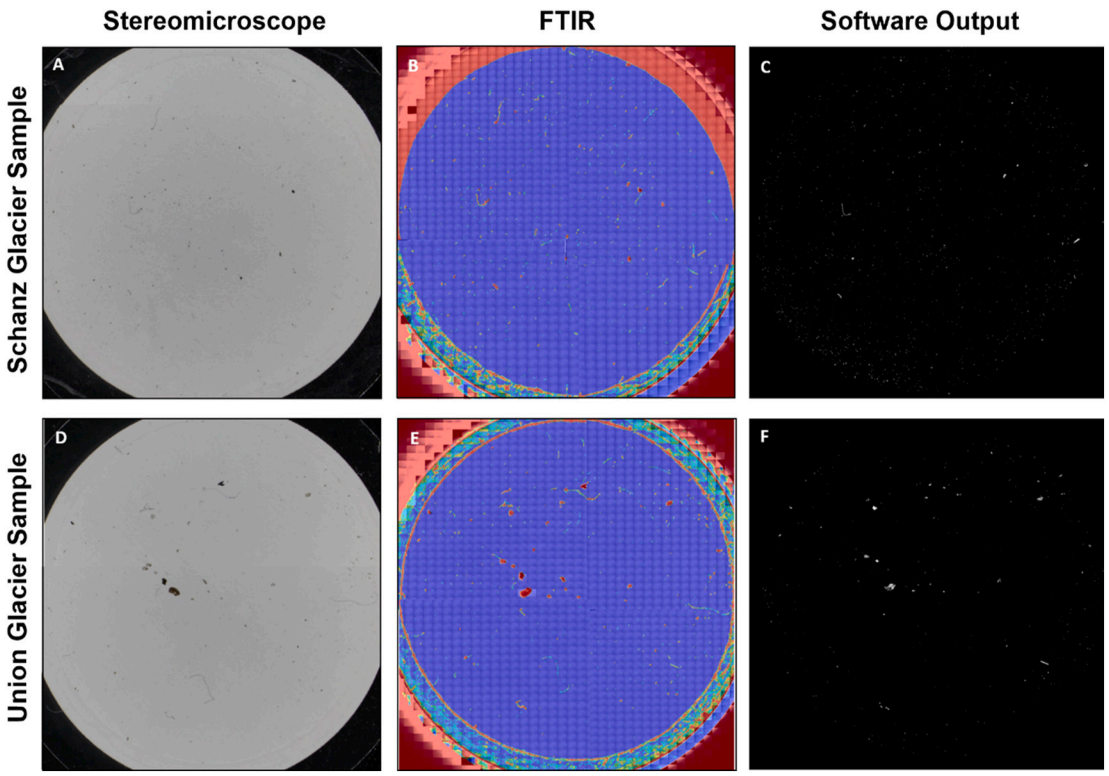

Fig. 3. Photographs illustrating the process of analysis from initial viewing using the Olympus stereomicroscope (A, D), the original FTIR heat-maps (B, E) highlighting regions of infrared absorption (red) using the Agilent spectrometer and the final software output (C, F) having matched spectra to the reference library. The two sets of images (A-C, D-E) show two random samples; Schanz-Glacier-4 (SG4) and Union Glacier-5 (UG5).

Anodisc® filter with on top to press the material on the surface into the focal plane.

All measurements were carried out using the Agilent 670 Fourier Transform Infrared (FTIR) spectrometer (Agilent Technologies, Santa Clara, CA), USA, with a cryogenically cooled mercury cadmium telluride (MCT) detector. The spectrometer was coupled to an Agilent 620 microscope with an automated XYZ-stage and 128 × 128 focal plane array (FPA) detector, cooled with liquid nitrogen. The FTIR system was continuously purged using a dry air generator (FGSR). The FTIR microscope was equipped with a 15 x IR objective lens and a 15-x visual objective lens. This stage held the sample in a bespoke filter holder enabling the transmission of infrared through the lower Cassegrain, the base of an Anodisc® filter where the sample was held, and through the Barium fluoride slide of the same shape and diameter as the filter. This setup facilitated FTIR imaging of both fibres and particles (microplastics of all other morphologies) (Primpke et al., 2019; Roscher et al., 2021).

Filters were scanned in quarters, with each quarter measuring approximately 14 mm × 14 mm to allow a small overlap between scans when stitching together the data. The FPA detector enabled each quarter to be scanned, acquiring a mosaic of spectra (Primpke et al., 2017, 2020a). This was calibrated with an XYZ stage allowing the exact co-ordinates at the end of the scan to be used to accurately identify the start of the next scanning area, covering the complete area of each filter (diameter of 25 mm, area 625 mm^2) (Fig. 3B, E). The collection of multiple mosaics meant each sample took approximately 13 scannable hours spread over 2.5 days.

The Resolution Pro software, inbuilt with the Agilent μFTIR setup, was used to collect 16 co-added scans of each filter with 8 cm^{-1} spatial resolution, binned at four intervals. Before each sample scan, a background scan was collected on the clean window in the same spectral range, comprising 64 co-added scans.

2.5. Data Processing and analysis

The data was exported, and the x,y matrix of spectral data, with 5.5 μm pixel resolution for each spectrum were analysed according to Primpke et al. (2020a). The siMPle software (version 1.1.ß) combined with MicroPlastic Automated Particle/fibre analysis Pipeline (MPAPP) (Primpke et al., 2019) enables the assessment of both particles and fibre-like microplastics (minimum 3:1 length to diameter). siMPle coupled with the Agilent FTIR, has been demonstrated to yield correct assignment rates (>95 %) when compared with commercial software tools existing at the time such as Bruker OPUS (Primpke et al., 2020a). siMPle is available open-access (www.simple-plastics.eu). Pixels in the region of the Anodisc® polypropylene ring were removed from the final sample calculations, with polyethylene and synthetic rubber also oversaturated in this region and subsequently removed. FTIR is considered most suitable to analyse MP ranging from 5 mm to ~10 μm (Primpke et al., 2020a), this lower detection limit aligns with the analytical capabilities of the FTIR used and therefore only microplastics 11 μm and above were analysed. Using the reference library of Primpke et al. (2018), each raw spectra and first derivative are compared with the reference database, using Pearson correlation. If both spectra match the same polymer, the polymer is successfully assigned and the combined hit quality indices (ranging from 600 to 2000) saved for future quality assurance (Primpke et al., 2017). The library (Primpke et al., 2018) also contains FTIR spectrum of natural materials such as coal, charcoal, natural polyamides, cellulose, quartz, and chitin. Concentrations of these materials are also reported in the results.

Normalised concentrations of all particles and fibres (Table S3) were calculated by subtracting the average concentration of each polymer and morphotype (fibre, particle) in the full procedural blanks from each raw sample concentration (Fig. S1). Concentrations are presented as both the extrapolated number of microplastics (MP) and mass of microplastics per litre of melted snow (MP L^{-1} and μg L^{-1} respectively)

(Bergmann et al., 2019). MP includes both particles and fibres. Concentrations for mass (μg) are calculated as part of the output from MPAPP (Simon et al., 2018), using the calculated surface area and reference polymer density as previously published (Primpke et al., 2020b).

2.6. Statistical analysis

Data were tested for normality using QQ plots and homoscedasticity was verified with box plots and residual plots. One-way ANOVAs with Tukey's post-tests were used to test for differences between (1) total microplastics, (2) individual polymer concentrations and (3) natural materials found at each site. To explore the possible compositional differences between sites, the polymer diversity for each site was also calculated using Shannon – Weiner diversity indices (H′). Looking at the samples ungrouped, Kendall Tau correlations were used to test for artefacts of sampling and analysis, by examining the correlation between polymer concentrations with (1) wind speed during sampling and (2) the corresponding laboratory blank concentrations.

3. Results

3.1. Microplastic in sub-surface snow

Microplastics were found in all samples, ranging from 73 MP L^{-1} at Schanz Glacier (SG2) to 3099 MP L^{-1} at Union Glacier (UG2) (Table 1 and table S3), with an average concentration of 817 ± 310 (SE) MP L^{-1} amongst all samples. There was no significant difference between the concentrations at the three sites (ANOVA, $F = 1.16$, $p = 0.37$) (Fig. 4a). Mean mass concentrations ranged from 3.6 ± 2.3 (SE) μg L^{-1} at the South Pole 32.2 ± 31.0 (SE) μg L^{-1} at Union Glacier. Similarly, there was no significant difference in the mass concentrations between sites (ANOVA, $F = 0.49$, $p = 0.66$) (Fig. 4c). Reporting the median instead there remains no significant difference between sites (Kruskall Wallis, $p = 0.57$).

Particles were the dominant shape, comprising 79 % of total microplastics, whilst fibres comprised only 21 %. Particles were found in all samples; fibres were found in 11/12 samples (table S4). Comparing between sites, fibres comprised 24 %, 21 % and 19 % in SP, UG, and SG respectively (Fig. 4B). There was no significant difference in the ratio of morphotypes between each site (ANOVA, $F = 2.35$, $p = 0.15$). The size of microplastic particles ranged between 11 and 497 μm. Fibre length ranged between 11 and 979 μm. Size distribution was skewed towards the smaller size fraction with 95 % of particles and fibres measuring <50 μm (Fig. 5).

In total, 14 different plastic polymers were found. The most common polymer was polyamide (PA), comprising 55.5 % of all microplastics found. This was followed by polyethylene terephthalate (PET) (12.3 %), polyethylene (PE) (10.9 %), synthetic rubber (10.3 %), acrylates/polyurethane varnish (4.6 %), polypropylene (3.1 %), chemically modified cellulose (CMC) (2.2 %), polyvinylchloride (PVC) (0.4 %), polystyrene (PS) (0.1 %) and ethylene vinyl acetate (EVA) (0.2 %). Other plastic polymers (nitrile rubber, polycarbonate (PC), polycaprolactone (PCL), polylactic acid (PLA), polyoxymethylene (POM)) comprised the remaining 1.1 %. There were between 2 and 10 different plastic polymers found in each sample (Fig. 6). The highest plastic polymer diversity was found at the South Pole (Shannon-Weiner Diversity, $H' = 1.82$), followed by Union Glacier and Schanz Glacier (Shannon-Weiner Diversity, $H' = 1.47$ and 1.04 respectively). The overall plastic polymer composition between the sites was not significantly different (ANOVA $F = 3.9, 0.99$, $p = 0.06$).

We explored the correlation between wind speed during sampling and microplastic concentration to provide additional insight into potential contamination of samples. Although there was no correlation between wind speed during sampling and overall microplastic concentration (Kendall Tau, $p = 0.35$), examining correlation for individual plastic polymers, revealed a correlation between synthetic rubber concentration and wind speed on the day of sampling (Kendall Tau, $p = 0.004$) (table S8). Removal of this polymer had no significant effect on the overall sample concentrations and subsequent analysis.

3.2. Microplastics at the control site and within technical replicates

Microplastics were found at the control site, although the lowest recorded in the sampling campaign (30 MP L^{-1}). This remote location also had the lowest plastic polymer diversity, with only POM ($n = 2$) and PP ($n = 28$) identified after normalisation, with all POM characterised as fibres and all PP as particles.

Two technical replicates were collected at the South Pole (SP3) (Table S3). These two samples contained similar proportions of fibres (28 % and 21 %), compared with particles, but varied considerably in final concentrations, recording 181 and 460 MP L^{-1} in each. Plastic polymer richness varied from 9 to 12, with EVA, PLA, and POM present in SP3b in very low concentrations (1.1 % of total MP concentration). SP3a was dominated by PE (26 %), PET (23 %) and synthetic rubber (21 %) followed by Acrylates (12 %) and PA (11 %). SP3b primarily comprised PA (26 %), Acrylates (26 %), PET (17 %) and synthetic rubber (9 %).

3.3. Other material

In addition to plastic polymers, particles and fibres of natural origin were also found across all sites and samples, comprising 53 %, 77 % and 83 % of total matter at Union Glacier, Schanz Glacier and the South Pole respectively (Fig. 7A). Concentrations were highest in Schanz Glacier (4060 ± (SE) 3342 n L^{-1}), followed by the South Pole (1887 ± (SE) 1662 n L^{-1}), and Union Glacier (808 ± (SE) 353 n L^{-1}), (Fig. 7B). These comprised plant fibres (natural cellulose), natural polyamides (furs), chitin, sand (quartz) and charcoal and coal (Fig. 7C). There was no correlation between the sampling parameters and the sample concentration (table S8).

3.4. Procedural blanks

The average concentration of the full procedural blank was 240 ± 49 (SE) MP L^{-1}. Polyamides comprised approximately 27 % of this total, followed by synthetic rubber (19 %), and PE and CMC (13 % each) (Fig. 8). Particles and fibres made up 75 % and 25 % of the total, respectively (Table S6). The subtraction of both fibres and particles (total microplastics) from each raw sample resulted in a reduction of between 22 % (SG4) and 86 % (SG2) (Table 2). The laboratory blank comprised fewer microplastics, with an average of 125 ± 13 (SE) MP L^{-1} with the most common plastic polymers being synthetic rubber (22 %), polyamide (19 %) and PET (17 %) (Fig. 8, Table S7). The laboratory blank comprised 89 % particles and 11 % fibres. PVC and "other" plastic polymers were absent from the blanks; however, a small amount of EVA (four particles in LB02) was identified.

Table 1
Summary statistics for Union Glacier (UG), Schanz Glacier (SG) and South Pole (SP) sites.

Statistic	Count concentration (MP L^{-1})			Mass concentration (μg L^{-1})		
	UG	SG	SP	UG	SG	SP
Minimum	84	73	152	0.34	0.57	0.16
Maximum	3098	2797	667	156.07	19.14	7.87
Median (SD)	152 ± 1328	929[a] ± 1232	322 ± 262	0.65 ± 69.26	2.93[a] ± 8.65	2.65 ± 3.94
Mean (SE)	723 ± 593	1182[a] ± 616	380 ± 152	32.19[a] ± 30.98	6.39 ± 4.32	3.56 ± 2.27

[a] Indicating the greatest concentration compared between sites using the same statistic and unit of measure.

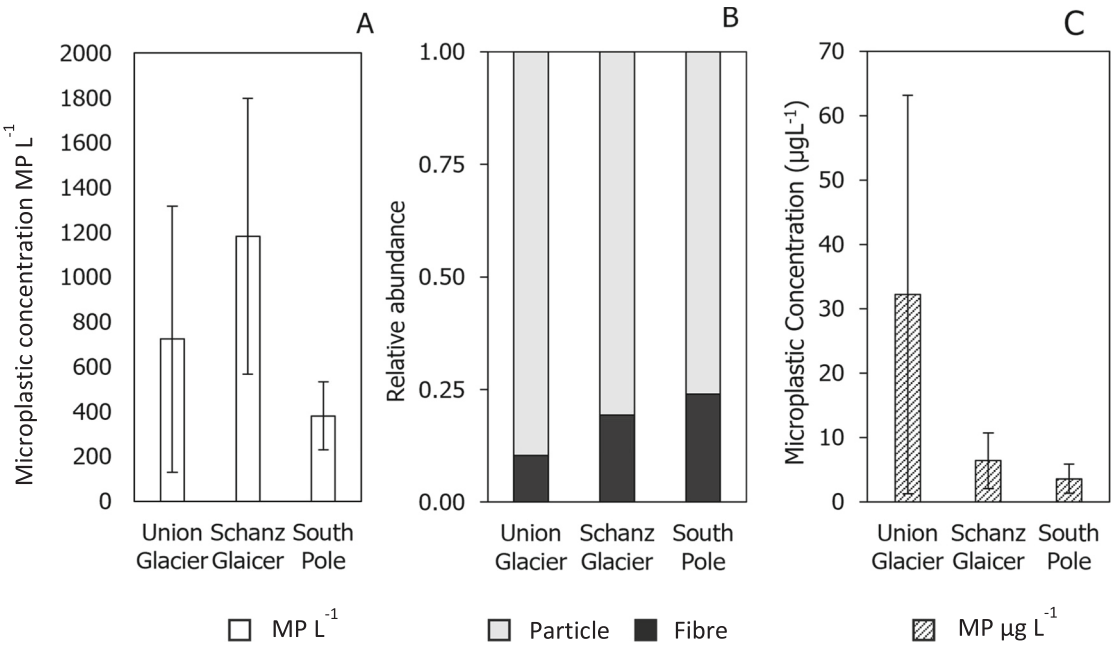

Fig. 4. Comparison of average microplastic concentrations at each site. A: Average microplastic concentration and standard error bars for each site, recorded as normalised counts MP L^{-1}. B: Relative abundance of particles and fibres. C: Average microplastic concentration and standard error bars recorded as mass (µg L^{-1}).

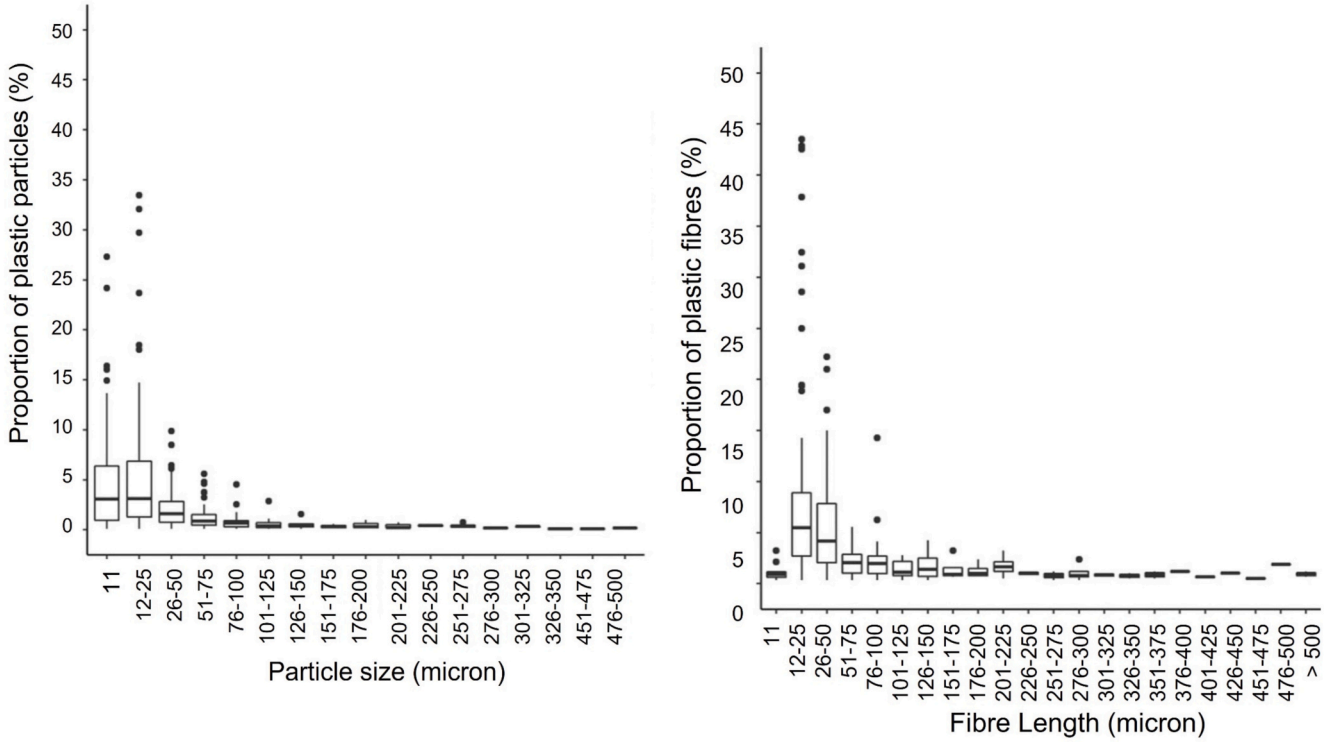

Fig. 5. Box and whisker plots indicating the proportion of (A) microplastic particles and (B) fibres in different size classes across all samples. The upper and lower boundaries of the box denote the 75th and 25th percentiles, respectively with median bars and black points showing outliers. The lower detection limit of analyses was 11 µm.

Natural particles were found in all blanks, with 998 ± 100 (SE) particles L^{-1} found in the full procedural blanks, comprising mostly of natural polyamides (55 %) and natural cellulose (37 %). Examination of the laboratory blanks individually shows an anomalously high concentration of natural particles and fibres in lab blank one (Table S6). The remaining two laboratory blanks comprised natural polyamides (66 %) and natural cellulose (25 %), with an average total concentration of 558 ± 146 n L^{-1}.

3.5. Recovery test

The results of the recovery tests (detailed in SI 4) indicate that the

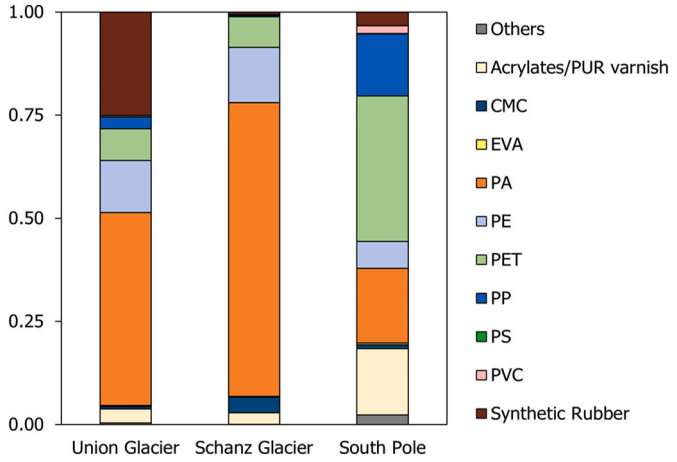

Fig. 6. Stacked histogram showing average polymer composition of each sample accord to FTIR analysis. Others: Nitrile rubber, POM = polyoxymethylene, PC = polycarbonate., PCL = polycaprolactone, and PLA = polylactic acid. CMC = chemically modified cellulose, EVA = ethylene vinyl acetate, PA = polyamide, PE = polyethylene, PET = polyethylene terephthalate, PP = polypropylene, PS = polystyrene, PVC = polyvinylchloride.

transference step resulted in a 99 % recovery rate (Table S9). The subsequent estimate of concentration provided by FTIR analysis, indicated a loss of 4–5 nylon fibres. No correction factor was used based on these results.

In the "clean snow" sample, 884 MP L^{-1} were found, comprising 76 % and 24 % particles and fibres respectively. Polyethylene terephthalate (PET) was the main plastic polymer, making up 32 % of the sample, followed by PVC (26 %) and Acrylates (17 %). Three particles of acrylonitrile butadiene styrene (ABS) were unique to this sample compared to all other snow samples (Table S3).

4. Discussion

A combination of FTIR imaging and automated polymer, particle and fibre identification revealed high concentrations of microplastics in regions of remote Antarctic camps. The average concentration of microplastics collected from the snow was two orders of magnitude higher (817 particles L^{-1}) than a previous study in East Antarctica (near MacMurdo research station) which averaged 29 particles L^{-1} (Aves et al., 2022). However, this study used automated FTIR imaging in Antarctic snow, enabling us to capture sizes down to 11 μm whilst Aves et al. (2022) manually sampled with μFTIR spectroscopy with a lower detection limit of 50 μm. The average microplastic particle concentration in the current study was similar to Bergmann et al. (2019) (625 particles L^{-1}), who also found predominantly small microplastics particles (95 % measuring <50 μm) in Arctic snow samples taken from Svalbard using similar automated FTIR techniques. We suggest that the size distribution of the particles shed light on the reason for the disparity between Aves et al. (2022) and the findings in this study. In fact, the concentration of microplastic observed in this study is reduced to 30 particles L^{-1} if only particles >50 μm are counted. The current study detecting approximately 100 times greater microplastic concentrations compared to Aves et al. (2022) highlights how microplastic in Antarctic snow may be of greater concern than previously thought. This has also recently been shown in Southern Ocean water samples with Leistenschneider et al. (2024) finding an exceptionally high concentration of microplastics compared to previous studies in the region, again attributing this to the ability to analyse small plastics down to 11 μm.

Measuring particles and fibres at a high resolution also yields high contamination of microplastic deetcted in the samples too, at least in part, due to the higher resolution of the analyses. Polyamide was found in approximately equal amounts in both procedural stages, accounting for 40 ± 9 % of each blank, and only PVC and ABS were absent from the samples. It is difficult to determine what the origins of these plastics are; however, a number of artefacts from the contamination library were verified as polyamide including flags, hand warmers and base layers and

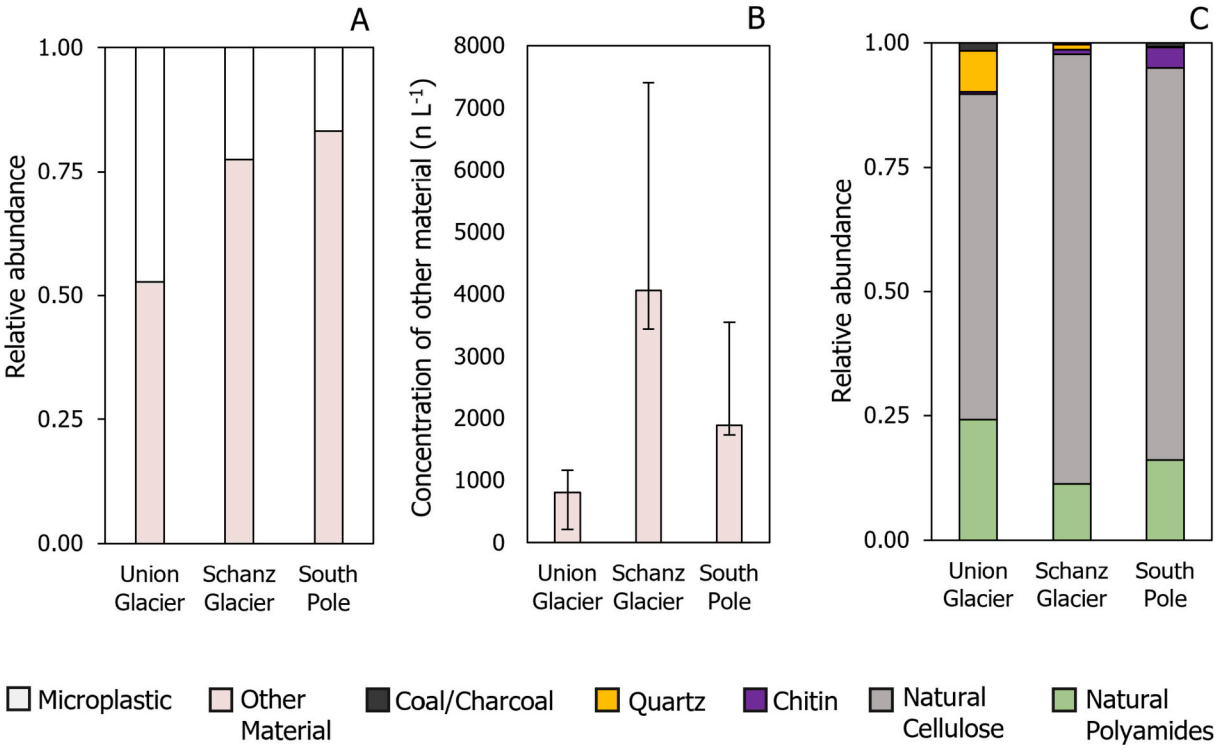

Fig. 7. Comparison of other material at each site. A: Relative abundance of microplastics and other material. B: Mean concentration of other material at each site, with error bars indicating standard error. C: Relative abundance of the composition of other material.

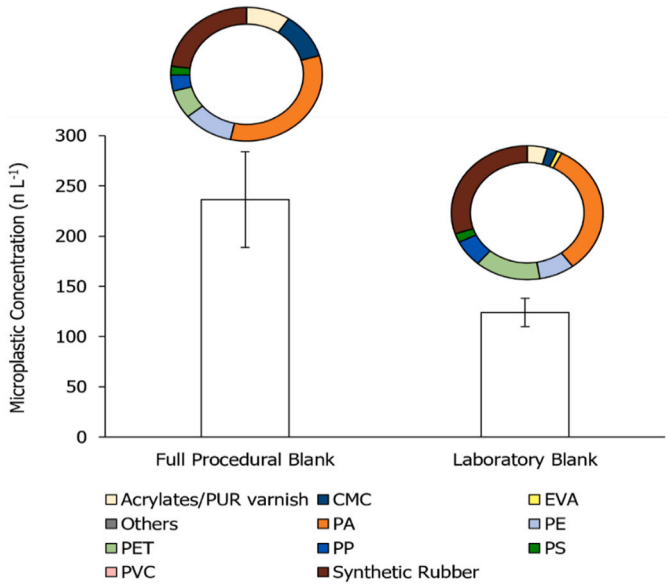

Fig. 8. A bar graph showing the measured mean concentration of microplastics in the full procedural blanks and laboratory blanks, with ring plots above each to show polymer composition.

Table 2
Raw microplastic concentrations and proportion of plastics in procedural blank yielding final MP concentration.

Sample	Total raw (MP L^{-1})	Total blank (MP L^{-1})	Normalised (MP L^{-1})	Blank fraction (%)
SG1	875	489	56 %	386
SG2	506	433	86 %	73
SG3	2113	640	30 %	1472
SG4	3575	777	22 %	2798
SP1	633	480	76 %	153
SP2	1293	628	49 %	666
SP3	1666	1024	61 %	642
UG2	4056	957	24 %	3099
UG3	473	388	82 %	85
UG4	606	441	73 %	165
UG5	525	409	78 %	116
UG1	543	392	72 %	151
C1 (control site)	158	128	81 %	30
"Clean snow"	1526	639	42 %	888

comparisons of full procedure and laboratory procedure blanks showed further contamination was introduced during the laboratory. Future work could incorporate adjustment of the cluster analysis using the data obtained from the contamination library (Roscher et al., 2021) and streamline processes in the laboratory.

This study found polyamide to be present at all sites with the maximum recorded at Schanz Glacier (SG4: 2185 MP L^{-1}), making up 78 % of the sample. Whilst Aves et al. (2022) also found Polyamide within samples taken from near McMurdo station in East Antarctica, it was not a significant proportion (6 %). Polyamide (including nylon) is mainly associated with textile fibres, and in these remote regions, localised sources are likely to come from technical clothing, ropes and the flags used to guide safe accessible routes, laid out at the beginning of each season. The ubiquity of polyamide within the camp proximal samples in our study and the absence from the remote site (control) could suggest that this is a local source of pollution. In snow samples taken from Terra Nova Bay, along the coast of the Northern Foothills near the Mario Zucchelli Antarctic research station, polyethylene and poly(ethylene-*co*-vinyl-acetate) were the predominant polymers identified which were also primarily in samples closest to the research base and as such were attributed to local pollution sources (Riboni et al., 2024). Aves et al. (2022) conversely found PET to be the most common polymer (79 % of all samples) which is the second most abundant polymer we identified too (12.3 %), but still much less than the polyamide which dominated. With similar methods in the Arctic, varnish (including acrylates) and rubber were the most common polymers identified which were highly variable across our samples (0–178.7 and 0–905.9 MP L^{-1} for Acrylates/PUR varnish and synthetic rubber respectively). In the current study, the greatest plastic polymer diversity was at the South Pole, which is the only permanent camp and may reflect a longer more persistent plastic footprint (Padha et al., 2022). Examining the temporal variation of microplastic pollution at each camp, during mobilisation, and operation would indicate the footprint of set-up compared to footfall whilst sampling over a wider geographical range could provide further information on local versus long-range sources.

The relative abundance of plastic polymer types found across our sample sites are concurrent with those found in other polar environments including glaciers (González-Pleiter et al., 2021), sea-ice (Peeken et al., 2018; Kelly et al., 2020) and sediments (Munari et al., 2017). Polyamide (PA), polyethylene terephthalate (PET), polyester (PE), acrylates and polyurethane, polypropylene (PP) and synthetic rubbers are the major plastic polymers found in the cryosphere, and this is reflected in the samples investigated here. Since cryosphere locations are often remote and far from heavily populated microplastic emission sources, they may also be considered a temporal sink for atmospheric microplastics (Zhang et al., 2023; Gaylarde et al., 2023; Hoffmann et al., 2020a, 2020b). Preserving microplastics in the snow, these cryospheric regions are consequently critical future study sites for determining temporal fluxes in microplastic pollution.

Particles were the dominant shape, comprising 79 % of total microplastics in this study, whilst fibres made up only 21 %. Conversely, Aves et al. (2022) found fibres were the most dominant microplastic morphotype (61 %) in Antarctic snow samples. Disparities are likely associated with the different analytical techniques (automated versus manual respectively) between the studies. In Arctic snow, whilst Bergmann et al. (2019) used similar automated techniques to detect microplastics down to 11 μm, they were unable to distinguish between synthetic and natural fibres, subsequently grouping all fibres in microplastic counts, making it difficult to draw comparisons to findings in this study regarding microplastic morphology. However, in a study of microplastics in snowfall in a northern island of Japan, Ohno and Iizuka (2023) determined particles heavily dominated the morphotype (97 %) when using a lower microplastic detection limit of 30 μm. Like our findings, the smallest detectable microplastics were most commonly particles.

The concentration of microplastics did not significantly differ between the 3 sites, despite the large variability in terms of human footprint at the different locations. Conversely, Aves et al. (2022) found that the concentration of microplastics measured at base sites (47 ± 8 particles L^{-1}) was significantly higher on average than at remote sites (22 ± 4 particles L^{-1}). This disparity could be due to the methods of Aves et al. (2022) potentially favouring local sources of microplastic pollution due to microplastic detection being limited to larger sizes (> 50 μm), whilst the lower detectable size limit in this study allows more exploration of potential local and long-range sources. Chen et al. (2023) modelled hemisphereic-scale airborne microplastic from the mid-Northern Hemisphre to Antractica concluding that microplastics >20 μm (mean length 1004.8 ± 823.5& 166.2 ± 88.6 μm for fibres and particles respectively) can undergo long-range transport to remote regions with fibres having consistent concentrations across a long trans-hemispheric distance whilst fragments reduced from North to South. Regional atmospheric models in other areas have shown that larger microplastics >120 μm were likely from local sites whereas smaller plastics could efficiently be transported >1000 km due to larger surface

area to volume ratios and lower densities than surrounding dust particles (Long et al., 2022). Atmospheric transport modelling indicates that Antarctica is a net importer of microplastics, with the flux of microplastics from mismanaged plastic waste in the ocean transferring to the atmosphere at the Antarctic coast likely exceeding anthropogenic sources of microplastics on the continent (Brahney et al., 2021). The dominance of small particles and fibres, particularly <100 μm in the current study, indicates long-range transport as a means for deposition to remote locations (Bergmann et al., 2019; Zhang et al., 2019).

The ubiquity of polyamide within the camp proximal samples and abence from the remote site (control) would suggest there are also local sources of pollution. Localised wind-driven snowdrift responsible for the redistribution of microplastics cannot be excluded. As an example, the current study observed highly localised microplastic concentration variation akin to the local variation in snow accumulation in this region (Hoffmann et al., 2020a, 2020b) resulting from near-surface winds (Picard et al., 2019). The relationship between microplastic's size and their atmospheric residence time and deposition are for the most part, poorly understood. To determine whether microplastics in Antarctic snow are driven by local sites, by long-range transport, or a combination of the two, further research is required. Utilising a larger spatial coverage, with more remote locations and a greater temporal coverage can aid in determining the correlation between concentration and proximity to camp.

The high abundance of microplastics in Antarctic snow found in this study may have wider climatic and ecological implications. Of particular concern, the light-absorbing properties of microplastics have recently been suggested to cause major changes in the albedo of snow and therefore the melt rate of cryospheric regions (Revell et al., 2021; Zhang et al., 2022). The high abundance of microplastics identified within Antarctic snow in the current study highlights the need for additional work to decipher microplastics' influence on snow and ice in these regions. Regarding ecological implications, samples have been collected in areas where strong katabatic winds can redistribute surface snow (Picard et al., 2019; Hoffmann et al., 2020a, 2020b) and therefore have the potential to transport microplastics from the near-surface, long distances across Antarctica, as recently modelled by Aves et al. (2022). Following the katabatic winds, 86 km to the edge of the Ronne Filchner Ice shelf, numerous penguin colonies exist with stable populations persisting for the last 65 years (Orgeira et al., 2021). Microplastics, predominantly polyethylene and PET, have been found in several penguin species, including Gentoo (Bessa et al., 2019), King (Le Guen et al., 2020), Adelie, and Chinstrap (Fragão et al., 2021). Microplastics released from remote sites could be transported to areas of high ecological importance. There is increasing evidence for uptake by Antarctic biota at different trophic levels (Wilkie-Johnston et al., 2023; Fragão et al., 2021). For example, the scat of varying seal species from the Peninsula was recently found to contain plastic polymers including polystyrene, polyester, PET, polyamide and polypropylene (Cebuhar et al., 2024) whilst in Antarctic fish species, polyamide was one of the predominant microplastic polymers identified, as well as polypropylene and polyethylene (Zhu et al., 2023). The findings of the current study suggest that remote camps present a risk of plastic pollution not currently accounted for in the environmental legislation of the region.

5. Conclusion

This study shows that anthropogenic activities are leaving a considerable microplastic footprint in Antarctic snow, with the concentrations in this study being considerably higher than previously recorded in remote Antarctica. There is currently no benchmark to determine what this plastic footprint is and whether it varies amongst the size of research bases. Hence, remote camps should be monitored for microplastic pollution and actions to reduce this footprint should be taken. On a broader scale, the findings of this study, i.e., high microplastic concentrations at the most remote and sensitive region of earth, magnify the need for collaborative, global plastic pollution mitigation strategies.

CRediT authorship contribution statement

Kirstie Jones-Williams: Writing – review & editing, Writing – original draft, Visualization, Software, Methodology, Investigation, Formal analysis, Data curation, Conceptualization. **Emily Rowlands:** Writing – review & editing, Software, Methodology, Data curation. **Sebastian Primpke:** Writing – review & editing, Software, Methodology, Formal analysis, Data curation. **Tamara Galloway:** Writing – review & editing, Supervision, Funding acquisition. **Matthew Cole:** Writing – review & editing, Supervision. **Claire Waluda:** Writing – review & editing, Supervision. **Clara Manno:** Writing – review & editing, Visualization, Supervision, Project administration, Funding acquisition, Conceptualization.

Declaration of competing interest

The authors declare that they have no known competing financial interests or personal relationships that could have appeared to influence the work reported in this paper.

Acknowledgements

K.J.W and all fieldwork was supported and financed by Airbnb. Special thanks to Lena Sönnichsen for her help in the field set-up. K.J.W also acknowledges Antarctic Logistics and Expeditions and partners including INACH and Universidad for Magellanes for their support in the programme, as well as the citizen science group, Vivek, Rasha, Tia, Kjersti and Spencer. S.P. was supported under the framework of JPI Oceans by the German Federal Ministry of Education and Research (Project FACTS - Fluxes and Fate of Microplastics in Northern European Waters; BMBF grant 03F0849A) and from the European Union's Horizon 2020 Coordination and Support Action programme under Grant agreement 101003805 (EUROqCHARM). This output reflects only the authors view and the European Union cannot be held responsible for any use that may be made of the information contained therein. The research falls under the framework of CalcUlating the strength of the Plastic pump In counteracting the Deep export of Oceanic carbon (CUPIDO) (UKRI-FLF project CUPIDO (MR/T020962)).

Appendix A. Supplementary data

Supplementary data to this article can be found online at https://doi.org/10.1016/j.scitotenv.2025.178543.

Data availability

All data is available at NERC EDS UK Polar Data Centre (https://doi.org/10.5285/ac6ade29-2815-4938-a93a-d84f0d322bd6).

References

Allen, S., Allen, D., Phoenix, V.R., Le Roux, G., Durántez Jiménez, P., Simonneau, A., Binet, S., Galop, D., 2019. Atmospheric transport and deposition of microplastics in a remote mountain catchment. Nat. Geosci. 12, 339–344. https://doi.org/10.1038/s41561-019-0335-5.

Allen, S., Allen, D., Moss, K., Le Roux, G., Phoenix, V.R., Sonke, J.E., 2020. Examination of the ocean as a source for atmospheric microplastics. PLoS One 15 (5), e0232746.

Allen, D., Allen, S., et al., 2022. Microplastics and nanoplastics in the marine-atmosphere environment. Nature Reviews Earth & Environment 3 (6), 393–405.

Aves, A.R., Revell, L.E., Gaw, S., Ruffell, H., Schuddeboom, A., Wotherspoon, E., Larue, M., Mcdonald, A.J., 2022. First evidence of microplastics in Antarctic snow. Cryosph 1–31.

Barker, P., Filippelli, G., Florindo, F., Martin, E., Scher, H., 2007. Onset and role of the Antarctic circumpolar current. Deep-Sea Res. II Top. Stud. Oceanogr. 54 (21–22), 2388–2398. https://doi.org/10.1016/j.dsr2.2007.07.028.

Bergmann, M., Mützel, S., Primpke, S., Tekman, M.B., Trachsel, J., Gerdts, G., 2019. White and wonderful? Microplastics prevail in snow from the Alps to the Arctic. Sci. Adv. 5, eaax1157. https://doi.org/10.1126/sciadv.aax1157.

Bessa, F., Ratcliffe, N., Otero, V., Sobral, P., Marques, J.C., Waluda, C.M., Trathan, P.N., Xavier, J.C., 2019. Microplastics in gentoo penguins from the Antarctic region. Sci. Rep. 9, 1–7. https://doi.org/10.1038/s41598-019-50621-2.

Brahney, J., Mahowald, N., Prank, M., Cornwell, G., Klimont, Z., Matsui, H., Prather, K. A., 2021. Constraining the atmospheric limb of the plastic cycle. Proc. Natl. Acad. Sci. U. S. A. 118 (16). https://doi.org/10.1073/PNAS.2020719118/-/DCSUPPLEMENTAL.

Cai, M., Yang, H., Xie, Z., Zhao, Z., Wang, F., Lu, Z., Sturm, R., Ebinghaus, R., 2012. Per- and polyfluoroalkyl substances in snow, lake, surface runoff water and coastal seawater in Fildes Peninsula, King George Island, Antarctica. J. Hazard. Mater. 209–210, 335–342. https://doi.org/10.1016/j.jhazmat.2012.01.030.

Cebuhar, J., Negrete, J., Rodríguez Pirani, L., Picone, A., Proietti, M., Romano, R., Della Védova, C., Casaux, R., Secchi, E., Botta, S., 2024. Anthropogenic debris in three sympatric seal species of the Western Antarctic Peninsula. Sci. Total Environ. 922, 171273. https://doi.org/10.1016/j.scitotenv.2024.171273.

Chen, Q., Shi, G., Revell, L.E., Zhang, J., Zuo, C., Wang, D., Le Ru, E.C., Wu, G., Mitrano, D.M., 2023. Long-range atmospheric transport of microplastics across the southern hemisphere. Nat. Commun. 14 (1), 7898. https://doi.org/10.1038/s41467-023-43695-0. PMID: 38036501; PMCID: PMC10689495.

COMNAP, 2022. COMNAP Antarctic Facilities. Available at: COMNAP Antarctic Facilities. arcgis.com. (Accessed 10 December 2022).

Fan, W., Salmond, J.A., Dirks, K.N., Cabedo Sanz, P., Miskelly, G.M., Rindelaub, J.D., 2022. Evidence and mass quantification of atmospheric microplastics in a coastal New Zealand City. Environ. Sci. Technol. 56 (24), 17556–17568.

Fragão, J., Bessa, F., Otero, V., Barbosa, A., Sobral, P., Waluda, C.M., Guímaro, H.R., Xavier, J.C., 2021. Microplastics and other anthropogenic particles in Antarctica: using penguins as biological samplers. Sci. Total Environ. 788, 147698. https://doi.org/10.1016/j.scitotenv.2021.147698.

Fraser, C.I., Kay, G.M., Plessis, M. du, Ryan, P.G., 2016. Breaking down the barrier: dispersal across the Antarctic Polar Front. Ecography (Cop.). 40, 235–237. https://doi.org/10.1111/ecog.02449.

Galloway, Tamara S., Cole, M., Lewis, C., 2017. Interactions of microplastic debris throughout the marine ecosystem. Nat. Ecol. &Amp; Evol. 1, 116. https://doi.org/10.1038/s41559-017-0116.

Gaylarde, C., Neto, J., Fonseca, E., 2023. Open access review microplastics in the cryosphere –a potential time bomb? Water Emerg. Contam. Nanoplastics 2 (4), 20. https://doi.org/10.20517/wecn.2023.27.

González-Pleiter, M., Lacerot, G., Edo, C., Pablo Lozoya, J., Leganes, F., Fernandez-Pinas, F., Rosal, R., Teixeira-De-Mello, F., 2021. A pilot study about microplastics and mesoplastics in an Antarctic glacier. Cryosphere 15, 2531–2539. https://doi.org/10.5194/tc-15-2531-2021.

Grant, S., Waller, C., Morley, S., Barnes, D., Brasier, M., Double, M., Griffiths, H., Hughes, K., Jackson, J., Waluda, C., Constable, A., 2021. Local drivers of change in southern ocean ecosystems: human activities and policy implications. Sec Conservation and Restoration Ecology 9. https://doi.org/10.3389/fevo.2021.624518.

Hoffmann, L., Eggers, S.L., Allhusen, E., Katlein, C., Peeken, I., 2020a. Interactions between the ice algae Fragillariopsis cylindrus and microplastics in sea ice. Environ. Int. 139. https://doi.org/10.1016/j.envint.2020.105697.

Hoffmann, K., Fernandoy, F., Meyer, H., Thomas, E.R., Aliaga, M., Tetzner, D., Freitag, J., Opel, T., Arigony-Neto, J., Florian Göbel, C., Jaña, R., Rodríguez Oroz, D., Tuckwell, R., Ludlow, E., Mcconnell, J.R., Schneider, C., 2020b. STable water isotopes and accumulation rates in the Union Glacier region, Ellsworth Mountains, West Antarctica, over the last 35 years. Cryosphere 14, 881–904. https://doi.org/10.5194/tc-14-881-2020.

IAATO, 2021. Tourism statistics-IAATO. Available at https://iaato.org/tourism-statistics.

Kelly, A., Lannuzel, D., Rodemann, T., Meiners, K.M., Auman, H.J., 2020. Microplastic contamination in east Antarctic sea ice. Mar. Pollut. Bull. 154, 111130. https://doi.org/10.1016/j.marpolbul.2020.111130.

Lazzara, M.A., Keller, L.M., Markle, T., Gallagher, J., 2012. Fifty-year Amundsen-Scott South Pole station surface climatology. Atmos. Res. 118, 240–259. https://doi.org/10.1016/j.atmosres.2012.06.027.

Le Guen, C., Suaria, G., Sherley, R.B., Ryan, P.G., Aliani, S., Boehme, L., Brierley, A.S., 2020. Microplastic study reveals the presence of natural and synthetic fibres in the diet of King Penguins (Aptenodytes patagonicus) foraging from South Georgia. Environ. Int. https://doi.org/10.1016/j.envint.2019.105303.

Leistenschneider, C., Wu, F., Primpke, S., Gerdts, G., Burkhardt-Holm, P., Gesellschaft, F. A., Foundation, R., 2024. Unveiling high concentrations of small microplastics (11–500 μm) in surface water samples from the southern Weddell Sea off Antarctica. Sci. Total Environ. 927, 172124.

Long, X., Fu, T.M., Yang, X., Tang, Y., Zheng, Y., Zhu, L., Shen, H., Ye, J., Wang, C., Wang, T., Li, B., 2022. Efficient atmospheric transport of microplastics over Asia and adjacent oceans. Environ. Sci. Technol. 56 (10), 6243–6252.

Munari, C., Infantini, V., Scoponi, M., Rastelli, E., Corinaldesi, C., Mistri, M., 2017. Microplastics in the sediments of Terra Nova Bay (Ross Sea, Antarctica). Mar. Pollut. Bull. 122, 161–165. https://doi.org/10.1016/j.marpolbul.2017.06.039.

Obbard, R.W., Sadri, S., Wong, Y.Q., Khitun, A.A., Baker, I., Richard, C., 2014. Earth's Future Global warming releases microplastic legacy frozen in Arctic Sea ice Earth's Future. AGU Publ. 1–6. https://doi.org/10.1002/2014EF000240.

Ohno, H., Iizuka, Y., 2023. Microplastics in snow from protected areas in Hokkaido, the northern island of Japan. Sci. Rep. 13 (1). https://doi.org/10.1038/S41598-023-37049-5.

Orgeira, J.L., Alvarez, F., Salvó, C.S., 2021. The same pathway to the Weddell Sea birdlife, after 65 years: similarities in the species composition, richness and abundances. Czech Polar Reports 11 (2), 291–304. https://doi.org/10.5817/CPR2021-2-20.

Padha, S., Kumar, R., Dhar, A., Sharma, P., 2022. Microplastic pollution in mountain terrains and foothills: a review on source, extraction, and distribution of microplastics in remote areas. Environ. Res. 207, 112232. https://doi.org/10.1016/J.ENVRES.2021.112232.

Peeken, I., Primpke, S., Beyer, B., Gütermann, J., Katlein, C., Krumpen, T., Bergmann, M., Hehemann, L., Gerdts, G., 2018. Arctic sea ice is an important temporal sink and means of transport for microplastic. Nat. Commun. 9, 1505. https://doi.org/10.1038/s41467-018-03825-5.

Picard, G., Arnaud, L., Caneill, R., Lefebvre, E., Lamare, M., 2019. Observation of the process of snow accumulation on the Antarctic Plateau by time lapse laser scanning. Cryosphere 13, 1983–1999. https://doi.org/10.5194/tc-13-1983-2019.

Potapowicz, J., Szumińska, D., Szopińska, M., Polkowska, Z., 2018. The influence of global climate change on the environmental fate of anthropogenic pollution released from permafrost. Sci. Total Environ. 651, 1534–1548. https://doi.org/10.1016/j.scitotenv.2018.09.168.

Primpke, S., Lorenz, C., Rascher-Friesenhausen, R., Gerdts, G., 2017. An automated approach for microplastics analysis using focal plane array (FPA) FTIR microscopy and image analysis. Anal. Methods 9, 1499–1511. https://doi.org/10.1039/C6AY02476A.

Primpke, S., Wirth, M., Lorenz, C., Gerdts, G., 2018. Reference database design for the automated analysis of microplastic samples based on Fourier transform infrared (FTIR) spectroscopy. Anal. Bioanal. Chem. 410, 5131–5141.

Primpke, S., Dias, P.A., Gerdts, G., 2019. Automated Identification and Quantification of Microfibres and Microplastics. https://doi.org/10.1039/c9ay00126c.

Primpke, S., Cross, R.K., Mintenig, S.M., Simon, M., Vianello, A., Gerdts, G., Vollertsen, J., 2020a. Toward the systematic identification of microplastics in the environment: evaluation of a new independent software tool (siMPle) for spectroscopic analysis. Appl. Spectrosc. 74, 1127–1138. https://doi.org/10.1177/0003702820917760.

Primpke, S., Fischer, M., Lorenz, C., Gerdts, G., Scholz-Böttcher, B.M., 2020b. Comparison of pyrolysis gas chromatography/mass spectrometry and hyperspectral FTIR imaging spectroscopy for the analysis of microplastics. Anal. Bioanal. Chem. 412, 8283–8298. https://doi.org/10.1007/s00216-020-02979-w.

Reed, S., Clark, M., Thompson, R.C., Hughes, K.A., 2018. Microplastics in marine sediments near Rothera Research Station, Antarctica. Mar. Pollut. Bull. 133, 460–463. https://doi.org/10.1016/j.marpolbul.2018.05.068.

Revell, L.E., Kuma, P., Le Ru, E.C., Somerville, W.R., Gaw, S., 2021. Direct radiative effects of airborne microplastics. Nature 598 (7881), 462–467.

Riboni, N., Ribezzi, E., Nasi, L., Mattarozzi, M., Piergiovanni, M., Masino, M., Bianchi, F., Careri, M., 2024. Characterization of small micro and nanoparticles in Antarctic snow by electron microscopy and Raman micro-spectroscopy. Appl. Sci. 14, 1597. https://doi.org/10.3390/app14041597.

Roscher, L., Halbach, M., Nguyen, M.T., Hebeler, M., Luschtinetz, F., Scholz-Böttcher, B. M., Primpke, S., Gerdts, G., 2021. Microplastics in two German wastewater treatment plants: yearlong effluent analysis with FTIR and Py-GC/MS. Sci. Total Environ. 817, 152619. https://doi.org/10.1016/j.scitotenv.2021.152619.

Rowlands, E., Galloway, T., Cole, M., Lewis, C., Peck, V., Thorpe, S., Manno, C., 2021. The effect of combined ocean acidification and nanoplastic exposures on the embryonic development of Antarctic krill. Front. Mar. Sci. 8. https://doi.org/10.3389/fmars.2021.709763.

Simon, M., van Alst, N., Vollertsen, J., 2018. Quantification of microplastic mass and removal rates at wastewater treatment plants applying Focal Plane Array (FPA)-based Fourier Transform Infrared (FT-IR) imaging. Water Res. 142, 1–9. https://doi.org/10.1016/J.WATRES.2018.05.019.

Sul, J.A., Barnes, D.K., Costa, M.F., Convey, P., Costa, E.S., Campos, L.S., 2011. Plastics in the Antarctic environment: are we looking only at the tip of the iceberg? Oecologia Australis 15, 150–170. https://doi.org/10.4257/OECO.2011.1501.11.

Taurozzi, D., Scalici, M., 2024. Seabirds from the poles: microplastics pollution sentinels. Front. Mar. Sci. 11, 1343617. https://doi.org/10.3389/fmars.2024.1343617.

Tejedo, P., Benayas, J., Cajiao, D., Leung, Y.-F., De Filippo, D., Liggett, D., 2022. What are the real environmental impacts of Antarctic tourism? Unveiling their importance through a comprehensive meta-analysis. J. Environ. Manag. 308. https://doi.org/10.1016/j.jenvman.2022.114634.

The Antarctic Treaty | Antarctic Treaty, 2023. Available at: https://www.ats.aq/e/antarctictreaty.html# (Accessed: January 2023).

Thompson, R.C., 2015. Microplastics in the marine environment: sources, consequences and solutions. In: Marine Anthropogenic Litter. Springer International Publishing, pp. 185–200. https://doi.org/10.1007/978-3-319-16510-3_7.

van Sebille, E., Aliani, S., Law, K.L., Maximenko, N., Alsina, J.M., Bagaev, A., Bergmann, M., Chapron, B., Chubarenko, I., Cózar, A., Delandmeter, P., Egger, M., Fox-Kemper, B., Garaba, P., Goddijn-Murphy, L., Hardesty, B.D., Hoffman, M.J., Isobe, A., Jongedijk, C.E., Kaandorp, M.L.A., Khatmullina, L., Koelmans, A., Kukulka, T., Laufkötter, C., Lebreton, L., Lobelle, D., Maes, C., Martinez-Vicente, V., Morales Maqueda, M.A., Poulain-Zarcos, M., Rodríguez, E., Ryan, P.G., Shanks, A.L., Shim, W.J., Suaria, G., Thiel, M., van den Bremer, T.S., Wichmann, D., 2020. The physical oceanography of the transport of floating marine debris. Environ. Res. Lett. 15 (2020), 023003. https://doi.org/10.1088/1748-9326/ab6d7d.

Wilkie-Johnston, L., Bergami, E., Rowlands, E., Manno, C., 2023. Organic or junk food? Microplastic contamination in Antarctic krill and salps. R. Soc. Open Sci. 10 (3), 221421. https://doi.org/10.1098/rsos.221421.

Zalasiewicz, J., Waters, C.N., Ellis, E.C., Head, M.J., Vidas, D., Steffen, W., Thomas, J.A., Horn, E., Summerhayes, C.P., Leinfelder, R., McNeill, J.R., Gałuszka, A.,

Williams, M., Barnosky, A.D., Richter, D. de B., Gibbard, P.L., Syvitski, J., Jeandel, C., Cearreta, A., Zinke, J., 2021. The Anthropocene: comparing its meaning in geology (Chronostratigraphy) with conceptual approaches arising in other disciplines. Earth's Future 9 (3), e2020EF001896. https://doi.org/10.1029/2020EF001896.

Zhang, Y., Gao, T., Kang, S., Sillanpää, M., 2019. Importance of atmospheric transport for microplastics deposited in remote areas. Environ. Pollut. 254. https://doi.org/10.1016/j.envpol.2019.07.121.

Zhang, Y.-L., Kang, S.-C., Gao, T.-G., 2022. Microplastics have light-absorbing ability to enhance cryospheric melting. Adv. Clim. Chang. Res. 13 (4), 455–458. https://doi.org/10.1016/j.accre.2022.06.005.

Zhang, Y., Gao, T., Kang, S., Allen, D., Wang, Z., Luo, X., Yang, L., Chen, J., Hu, Z., Chen, P., Du, W., Allen, S., 2023. Cryosphere as a temporal sink and source of microplastics in the Arctic Region. Geosci. Front. 14 (4). https://doi.org/10.1016/j.gsf.2023.101566.

Zhu, W., Zhao, N., Liu, W., Guo, R., Jin, H., 2023. Occurrence of microplastic in Antarctic fishes: abundance, size, shape and polymer composition. Sci. Total Environ. 10 (903), 166186. https://doi.org/10.1016/j.scitotenv.2023.166186.